

EXPLORING SEA-ICE THICKNESS WITHIN THE CCCMA CANESM5 MODEL

Alison Deere
ATSC448 - Directed Studies

Table of Contents

Summary	3
Motivation/Background	3
Motivation	3
Data Used	4
Analysis Techniques	6
Data Format	6
Qualitative Analysis	6
Estimating Natural Variability	6
Taylor Diagrams	7
Results	8
Historical Simulation	8
Future Scenarios	12
HadGEM3-GC3.1-LL	13
Comparison	15
Conclusion	19
References	20

Summary

Sea-ice thickness in the arctic is decreasing. As climate change continues to progress, both surface and sea temperatures will continue to rise. This will contribute to the melting of sea-ice, and impact communities and wildlife who depend on the sea-ice to survive. Within this directed studies research project, sea-ice thickness simulated by the Canadian Earth System Model version 5 will be analyzed. This model will be compared to the Hadley Centre Global Environment Model to determine if there are significant differences between the two. Quantitative and qualitative analyses are performed, extending to both the spatial and temporal extent of the sea-ice thickness models. Overall, the two models predict dramatic decreases in sea-ice thickness both in the historic simulation and in future emissions scenarios, and significant differences were found between the two models.

Motivation/Background

Motivation

It is a common belief “that climate change will be felt first —and to a greater extent—at high latitudes versus temperate regions” (Pickart, 2018). With climate change comes warmer temperatures, and a loss of sea-ice in the arctic. This loss of sea-ice will impact indigenous communities in Canada’s arctic who rely on sea-ice for transportation, as well as arctic marine mammals and fish as “staples of their traditional diets” (Panikkar & Lemmond, 2020). Accurate and extensive sea-ice models are very important, to both understanding how sea-ice has changed historically as well as looking into the future. These models can be used to influence policies around mitigation and helping local communities adapt to changing sea-ice conditions.

Sea-ice thickness and extent models are very important, but sea-ice can be a very difficult phenomenon to model due to the complex interaction of the Earth’s atmosphere and oceans. Often, the details in the model predictions do not agree with observations. However, at a macro scale, it has been observed in both models and observations, that arctic sea-ice area has “decreased rapidly” (Notz & Community, 2020) in recent decades as anthropogenic greenhouse gas emissions have continued to warm global temperatures.

The purpose of this directed studies research project is to analyze the Canadian Earth System Model Version 5 (CanESM5) from the Canadian Centre for Climate Modelling

and Analysis (CCCma) within phase 6 of the coupled model inter-comparison project (CMIP). In this project, both historic simulations from 1850-2014 and future emissions scenarios from 2015 to 2100 will be examined using various qualitative and quantitative methods. The CanESM5 model will be compared with the Hadley Centre Global Environment Model (HadGEM) from the Met Office Hadley Centre in the United Kingdom, using statistical Taylor diagrams.

Data Used

In this study, publicly available data was used from the sixth phase of the coupled model inter-comparison project, and focused on the CanESM5 and HadGE34-GC3.1-LL models. These are described in more detail below.

CanESM5

The Canadian Earth System Model version 5 is the current version of the Canadian Centre for Climate Analysis' global model. There were many improvements to the model between the last iteration (version 2), and the current model. The update includes improvements to the atmosphere, land surface, and terrestrial ecosystem models, and the implementation of completely new models for the ocean, sea-ice, and marine ecosystems (Swart et al., 2019).

Within CanESM5, the atmosphere is represented by the Canadian Atmosphere Model, which includes the Canadian Land Surface Scheme and the Canadian Terrestrial Ecosystem model. The ocean is simulated using the LIM2 sea-ice model which is run within the Nucleus European Modelling of the Ocean model (NEMO) framework. The ocean biogeochemistry is represented by the Canadian Model of Ocean Carbon. The atmosphere and the ocean components of this model are coupled by the Canadian Coupler, and LIM2 provides the sea-ice concentration, snow and ice thickness to the atmospheric model, via the coupler (Swart et al., 2019).

The CanESM5 model has a resolution of approximately 2.8° for the atmosphere, and 1° for the ocean (Swart et al., 2019). The spatial extent for the CanESM5 sea-ice model is 360 by 291 grid cells (longitude by latitude). In the historical simulations, there are 1980 time-steps ranging from 1850 to 2014, and in the future emissions scenarios there are 1032 time steps, ranging from 2015 to 2100.

The Canadian Earth system model has 40 ensemble members for the historical simulations of sea-ice thickness in CMIP6. These ensemble members were generated by launching historical runs at 50-year intervals off the pre-industrial configuration

simulation. The 50-year interval was chosen to allow for differences in multi-decadal ocean variability between ensemble members (Swart et al., 2019).

HadGEM3-GC3.1-LL

The Met Office Hadley Centre has three models in CMIP6. In this project, the focus will be on the HadGEM3-GC3.1-LL model and it will be used to perform a comparison with the CanESM5 model. The HadGEM3-GC3.1-LL model is the latest configuration of the Global Coupled model, and it includes component configurations Global Atmosphere 7.1, Global Land 7.0, Global Ocean 6.0, and Global Sea Ice 8.1 (Williams et al., 2018). The global sea ice component is embedded in the NEMO ocean configuration, and uses a tripolar grid. The atmosphere model and the ocean model are coupled by the OASIS-MCT coupler (Ridley et al., 2018). The HadGEM3-GC3.1-LL has four ensemble members with the intent of mitigating the “impact of model internal variability when analyzing the ensemble mean fields” (Andrews et al., 2020). The initial conditions for the historical simulation ensemble members were taken from a variety of points during the numerical integration of the pre-industrial configuration simulation run (Andrews et al., 2020).

Coupled Model Inter-comparison Projects

Coupled model inter-comparison projects are sets of model results that are released in the lead up to each intergovernmental panel on climate change assessment report. CMIP6 is associated with the IPCC sixth assessment report and consists of runs from around 100 climate models, produced across 49 different modelling groups. Within CMIP6 there are historical simulations as well as 22 specialized experiments or model inter-comparison projects, that modelling groups can choose to participate in (CMIP6, 2019). This project will focus on historical simulations, as well as the modelling inter-comparison project ScenarioMIP, which looks at future emissions scenarios.

Projections of future climate scenarios play an integral role in improving understanding of our climate system, and in the case of this research project, how sea-ice thickness will continue to change into the future. The scenario model inter-comparison project consists of 8 alternative 21st century scenarios. Each scenario represents a different representative concentration pathway (RCP). This project has focused on two: the SSP2-4.5 and SSP5-8.5 scenarios. SSP2-4.5 and SSP5-8.5 “are the middle and high end of the range of future forcing pathways, respectively, updating the RCP4.5 and RCP8.5 pathways” (Wei et al., 2020). RCP8.5 corresponds to the scenario of the highest level of greenhouse gas emissions. It stabilizes radiative forcing at 8.5 Wm^{-2} and is the worst case scenario (Riahi et al., 2011). RCP4.5 assumes that some climate policies are created

that limit the extent of greenhouse gas emissions, and stabilizes radiative forcing at 4.5 Wm⁻² (Thomson et al., 2011).

Analysis Techniques

Data Format

The data used for this research project came from CMIP6, and is in the format of xarray datasets with dask arrays of sea ice thickness, latitude, and longitude. All of the analysis techniques described below were implemented using the python programming language. Monthly sea-ice thickness projections for the CanESM5 and HadGEM3-GC3.1-LL models were used. The historical sea-ice thickness simulations covered the period from 1850 – 2014, and the future emissions scenarios covered the period from 2015–2100.

Qualitative Analysis

This research project began with a qualitative analysis of the data within CanESM5. The analysis focused on the entire spatial extent for a given snapshot in time, as well as the entire temporal extent looking at spatial averages of the model. To examine the entire spatial extent, two sets of polar plots were created. The first looks at one ensemble member and has the intent of showing how the polar sea-ice thickness has changed from 1850-2014. The second looks at all of the ensemble members within CanESM5 and is used to explore the variability in sea-ice thickness between the ensemble members.

These polar plots were created with the Matplotlib python library (Hunter, 2007), and a function was created to attempt to decrease the visible seam that is visible in the north pole. The polar plots show the extent from 60 degrees north to 90 degrees north. The temporal variation of sea-ice thickness was examined by calculating yearly means of area weighted sea-ice thickness.

Estimating Natural Variability

Given that the CanESM5 model has 40 ensemble members, we can use the variability between the models as an estimate of natural variability. There is variation between the ensemble members shown in the polar plot in Figure 3. To further explore this and to analyze the sea ice thickness trends without the internal variability between the different members, the ensemble mean and variability between models were calculated. These calculations were performed for the historical simulations of the CanESM5 and HadGEM3-GC3.1-LL models, as well as for the future emissions scenarios. Standard deviation was used as a measure for variability. The sea-ice thickness in Figure 4 is area-

weighted, only examines the sea ice north of the equator, and is calculated only with grid cells with a sea-ice thickness greater than zero. Figure 5 shows the spread of the variability between the models, calculated as the range of standard deviation.

Taylor Diagrams

To perform quantitative comparisons between the CanESM5 and HadGEM3-GC3.1-LL models, Taylor Diagrams were used. A Taylor diagram can “concisely summarize the degree of correspondence between simulated and observed fields” (Taylor, 2001). The Taylor diagram looks at three statistics: the correlation coefficient between the reference and model dataset, the centred pattern root-mean-square difference, and the standard deviation. The following two equations give the correlation coefficient (R) and the centred pattern root-mean-square difference (E) (Taylor, 2001).

$$R = \frac{\frac{1}{N} \sum_{n=1}^N (f_n - \bar{f})(r_n - \bar{r})}{\sigma_f \sigma_r}$$

$$E = \frac{1}{N} \sum_{n=1}^N [(f_n - \bar{f}) - (r_n - \bar{r})]^2$$

On a Taylor diagram, the spatial correlation between the reference dataset and the model dataset is given by the azimuthal position on the diagram, the centred pattern root-mean-square difference is proportional to the distance from the reference point on the x-axis, and the standard deviation is proportional to the radial distance from the origin. The Taylor diagrams for this project were created using the Skill Metrics python library (Rochford, 2021).

Results

Historical Simulation

The CMIP6 historical simulation ranges from 1850 to 2014. The following figure shows the CanESM5 model in its first time step (1850) on the left, and in its last time step (2014) on the right.

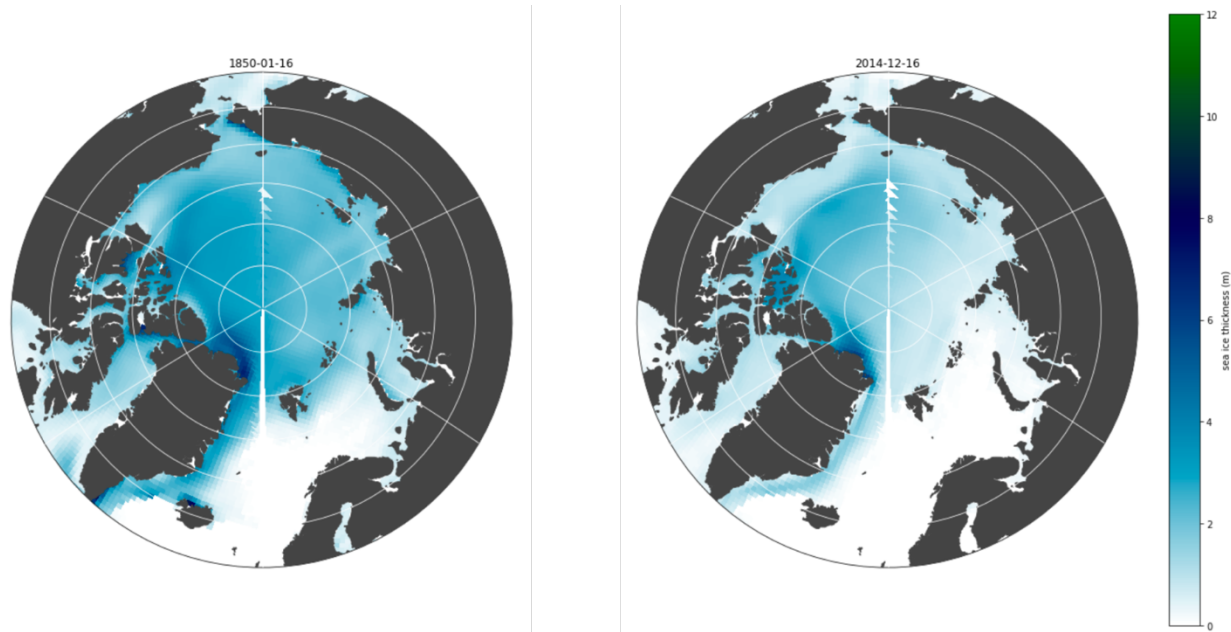


Figure 1: Polar Plots from 60 degrees north to 90 degrees north of one ensemble member (r1i1p2f1) within the CanESM5 model. The first time step (1850) is on the left, the las time step (2014) is on the right.

The above figure alone shows that the CanESM5 model predicts a decrease in sea-ice thickness from 1850 to 2014. On the left, the blue is darker over the ocean than on the right, which represents thicker sea-ice. To further analyze the loss of sea-ice thickness over the 164 year period, polar plots were created for every decade.

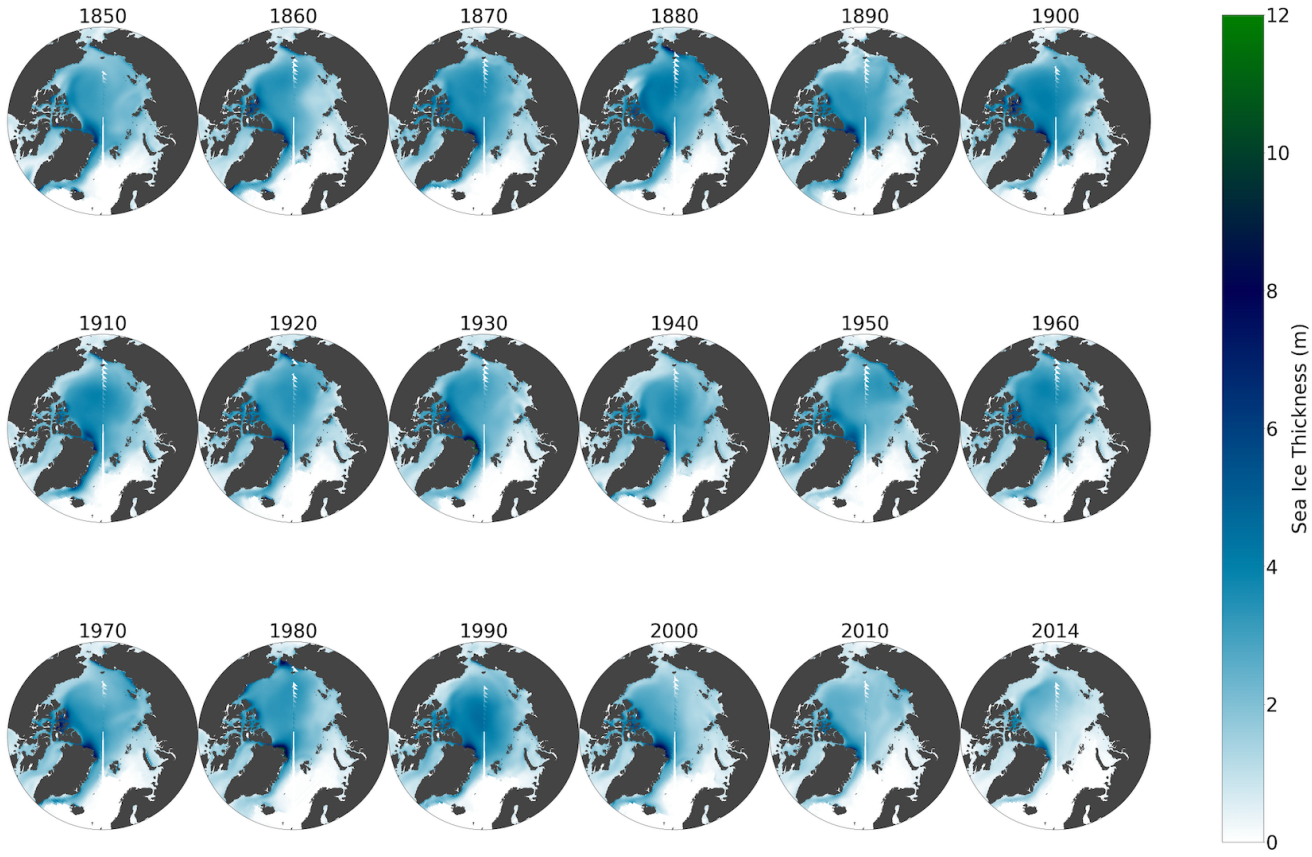


Figure 2: Polar Plots from 60 degrees north to 90 degrees north of one ensemble member (r1i1p2f1) within the CanESM5 model. Figures are from 1850 - 2014, with one plot every decade.

From Figure 2, we can see the changes in sea-ice thickness from 1850 to 2014. As the years go by, the sea-ice decreases, and in this figure, the ocean becomes lighter and lighter blue. As will be further discussed below, the sea-ice thickness was modelled to remain approximately constant in the arctic from 1850 - about 1970. In Figure 2, we can see qualitatively that the difference in the colour of blue from the 1850 plot (row 1, column 1) to the 1960 plot (row 2, column 6) is not that extreme. However, if we compare the 1970 plot (row 3, column 1) to the 2014 plot (row 3, column 6), there is a large difference in the shade of blue over the ocean. Most of the decrease in sea-ice thickness has occurred over the last 50 years. By 2014 the sea-ice in the middle of the arctic ocean is approximately 1-2 m thick. Figures 2 and 3 were created with only one ensemble member from the CanESM5 model. To look into the variability of all of the ensemble members within the model, an additional figure had to be created.

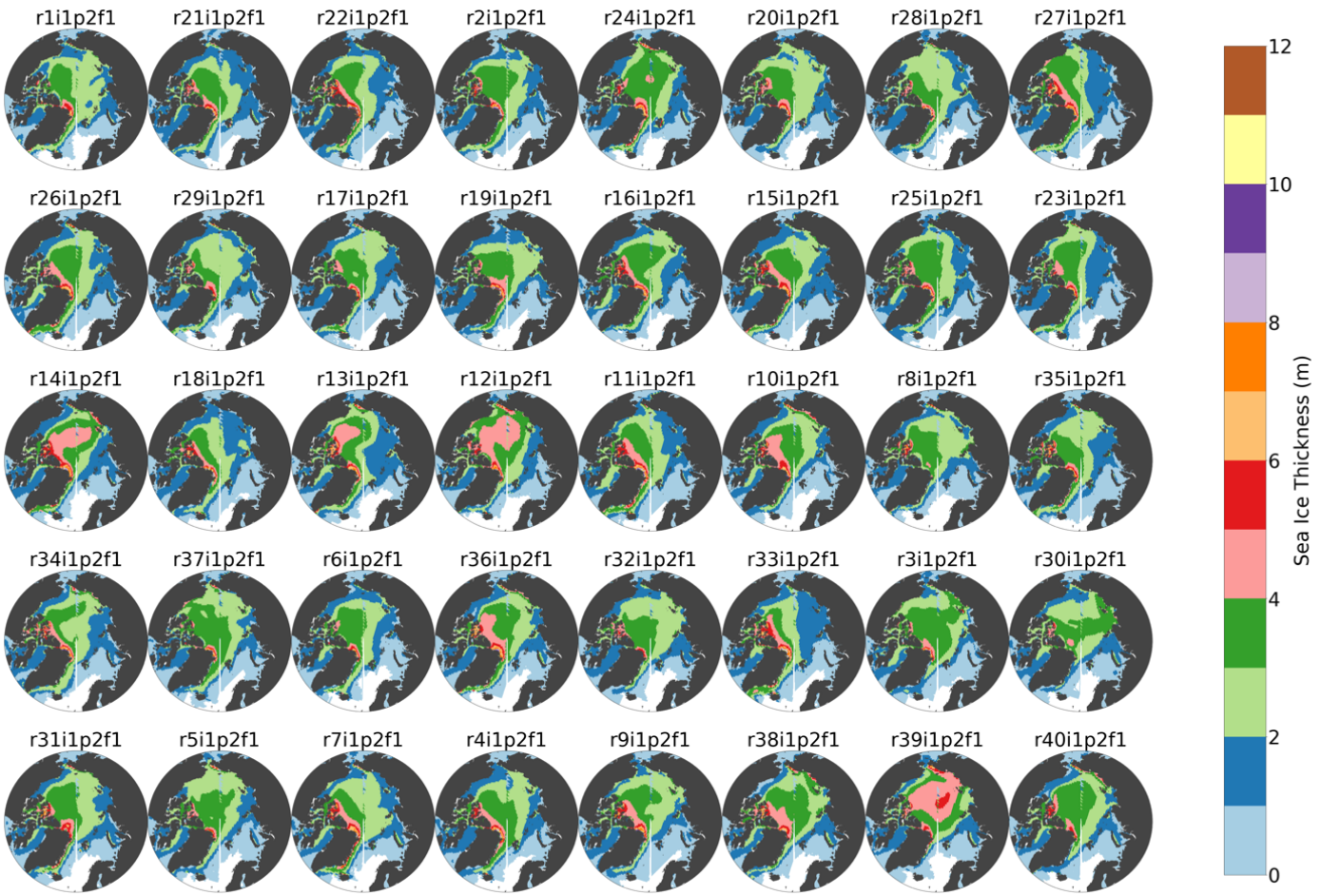


Figure 3: Polar Plots in 1850 from 60 degrees North to 90 degrees North for the 40 ensemble members within CanESM5.

Figure 3 shows all 40 of the ensemble members within CanESM5 in 1850. The qualitative colour scheme is chosen to showcase the variability between members. For example, ensemble member r39i1p2f1 (row5, column 7) has a much thicker sea-ice in the middle of the ocean. To further explore the variability within the model, area-weighted sea-ice thickness was calculated, along with the ensemble mean and standard deviation between the different ensemble members.

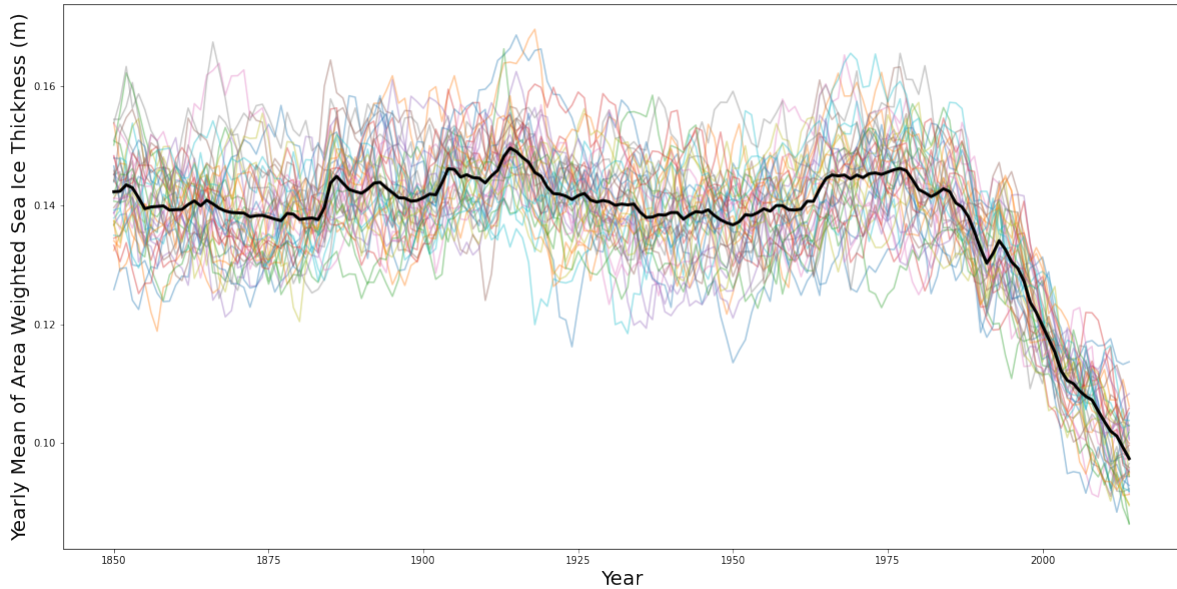


Figure 4: Area-weighted sea-ice thickness for areas north of the equator with sea-ice thickness above zero for the 40 ensemble members within the CanESM5 sea-ice thickness model.

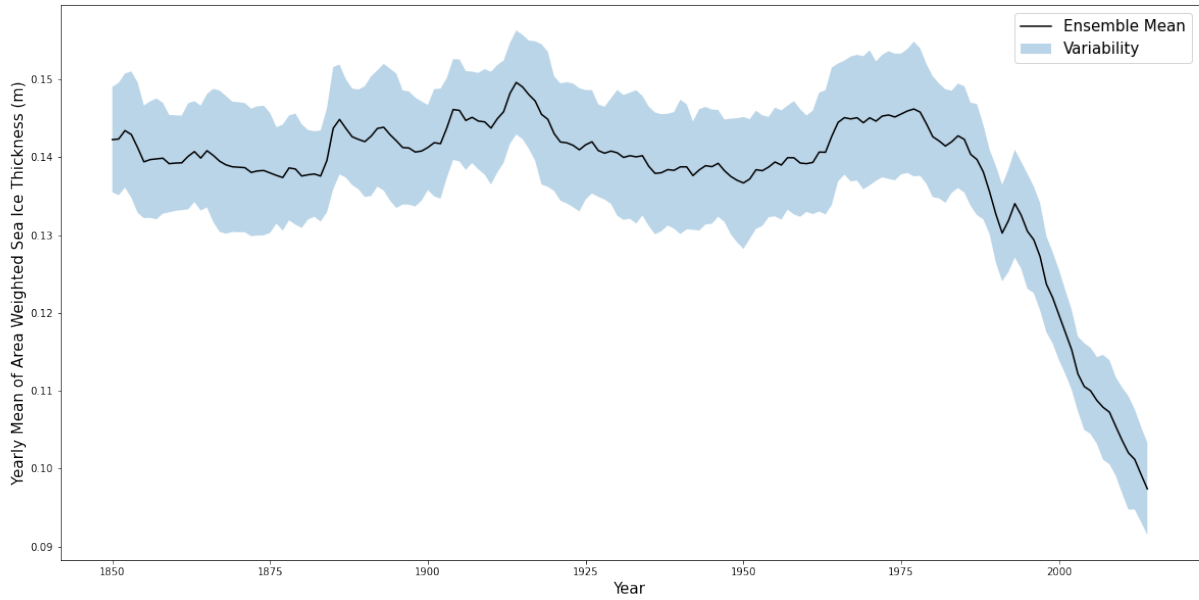


Figure 5: Ensemble mean of area-weighted sea-ice thickness for areas north of the equator with sea-ice thickness above zero with range of variability within the CanESM5 sea-ice thickness model.

Looking at ensemble member predictions can aid in separating long term climate effects from changes that are “inherent to the climate system” (Bengtsson & Hodges, 2019). Figure 4 clearly illustrates the decreasing trend of sea-ice thickness, with the greatest standard deviation being 0.0091 m. The thickness of sea-ice in Canada’s arctic has been decreasing since the model’s initialization in 1850. Time 1850 in this plot corresponds to

the ensembles examined in Figure 3. Figure 4 shows that while there is internal variability between the 40 ensemble members due to different initial conditions, the overall trend of sea-ice thickness is an almost linear decrease after approximately 1975. This was discussed earlier with the polar plots from 1850-2014, and the trend holds in these figures. From 1850 to 1975, the sea-ice thickness stayed approximately constant, around 0.14 m. After 1975, yearly mean of area weighted sea-ice thickness decreased dramatically. In the next section there is further analysis of the sea-ice thickness after 2014.

Future Scenarios

CMIP6's scenario model inter-comparison project has 8 alternative 21st century emissions scenarios. Figure 6 shows SSP2-4.5 and SSP5-8.5 in the CanESM5 model. It is clear that the trend that was noted in Figures 4 and 5 is set to continue into the future. Even with climate policies being enacted over the next 80 years, which the simulation SSP2-4.5 takes into account, there will be a dramatic decrease in sea-ice thickness.

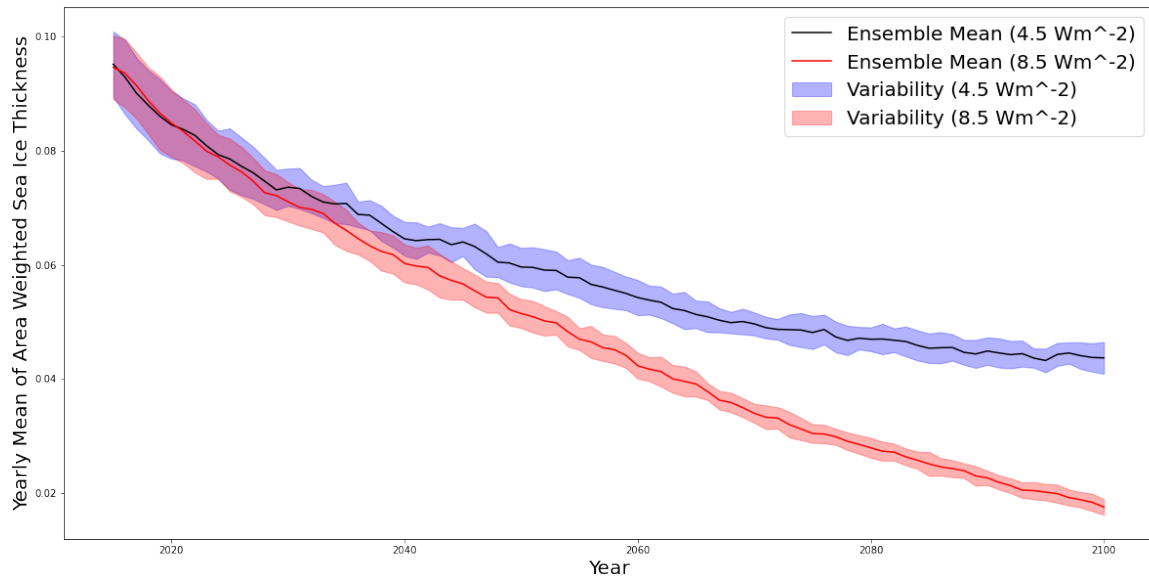


Figure 6: Ensemble mean of area-weighted sea-ice thickness for areas north of the equator with sea-ice thickness above zero with shaded variability for two future emissions scenarios within CanESM5

If the other emissions scenarios available within CMIP6 were plotted on Figure 6, they would bracket the blue curve and would all be above the red curve. If the SSP2-4.5 scenario becomes reality, then by 2100 the yearly mean of area weighted sea ice thickness would be around 0.05 m, and would be 0.02 m if the SSP5-8.5 scenario comes to fruition.

HadGEM3-GC3.1-LL

The Met Office Hadley Centre's HadGEM3-GC3.1-LL model was chosen to compare to the CCCma's CanESM5 sea-ice thickness model. Below are the four ensemble members that make up the HadGEM3-GC3.1-LL model in 1850.

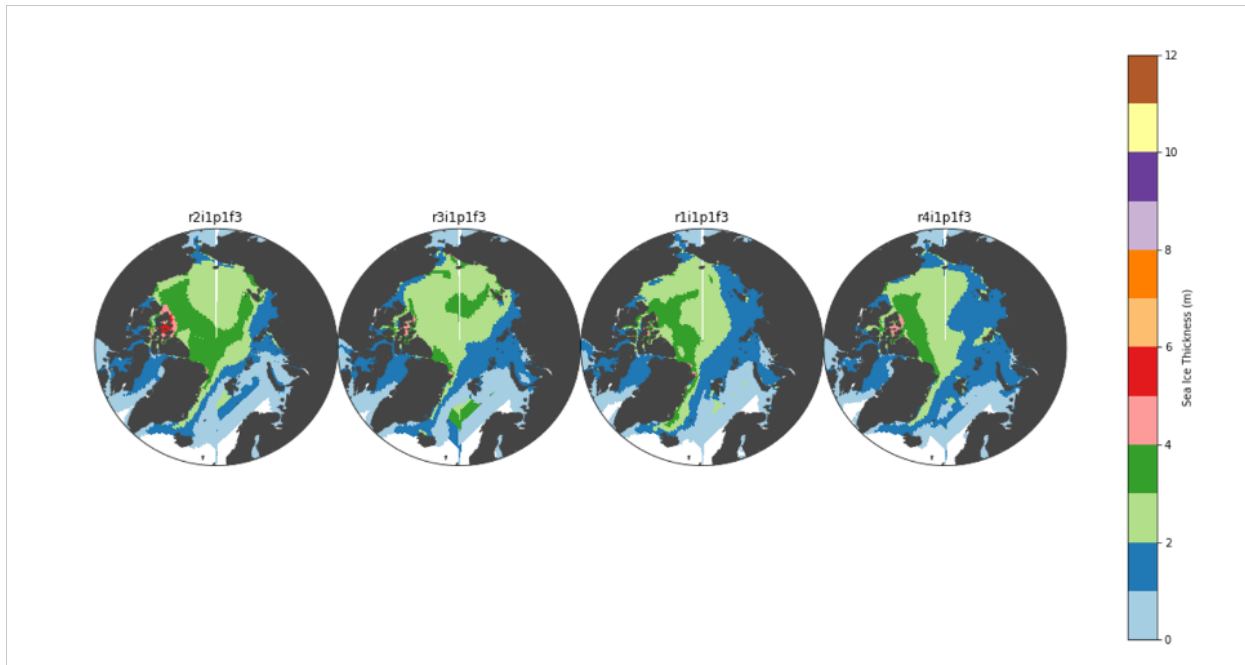


Figure 7: Polar Plots from 60 degrees north to 90 degrees north of the four ensemble members within HadGEM3-GC3.1-LL in 1850.

As with the CanESM5 polar plots above (Figure 3), there is internal variability between the models, though there is less overall variability. The arctic sea-ice for these four ensemble members in 1850 is approximately 2-4 m thick in the middle of the ocean. In Figure 3, there were ensemble members from the CanESM5 model that simulated sea-ice both thicker and thinner in areas than these four ensemble members. To further examine the HadGEM3-GC3.1-LL model in preparation to comparing it with the CanESM5 model, the ensemble mean and standard deviation were calculated.

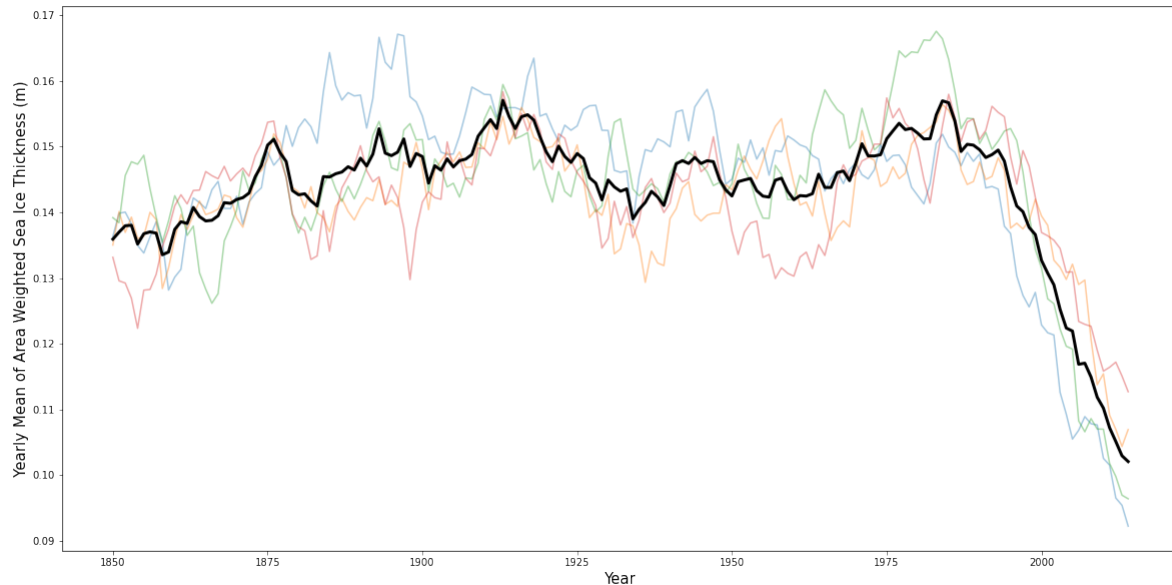


Figure 8: Area-weighted sea-ice thickness for areas north of the equator with sea-ice thickness above zero for the 4 ensemble members within the HadGEM3-GC3.1-LL sea-ice thickness model.

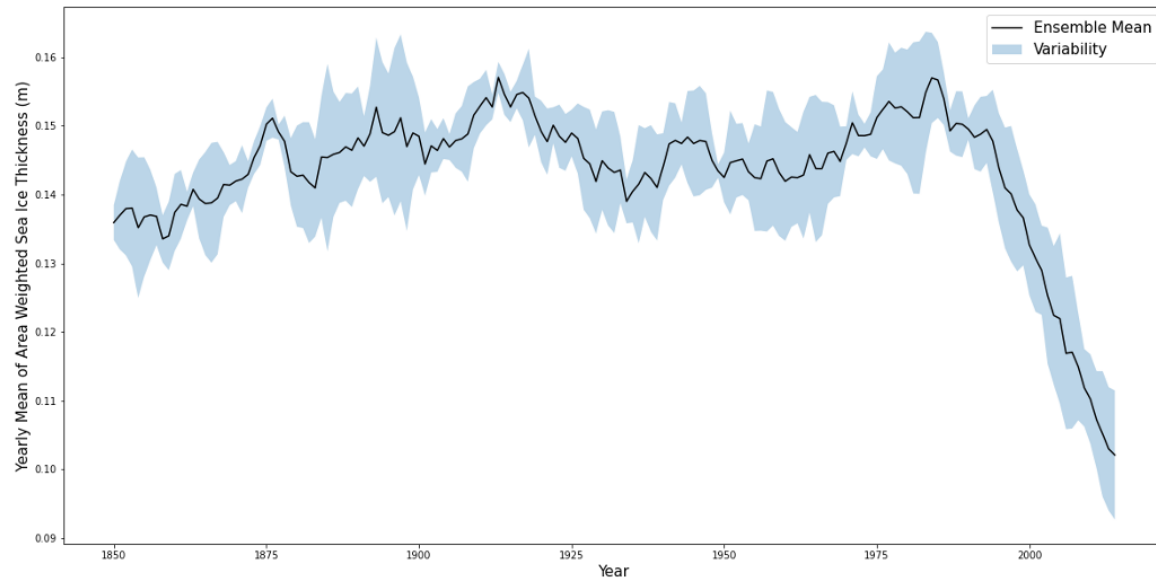


Figure 9: Ensemble mean of area-weighted sea-ice thickness for areas north of the equator with sea-ice thickness above zero with range of variability within the HadGEM3-GC3.1-LL sea-ice thickness model.

Similarly to the CanESM5 model's ensemble mean and variability figures, Figure 8 and Figure 9 highlight the variability between the ensemble members within the model. With only four ensemble members within the HadGEM3-GC3.1-LL model, there is less internal variability than within the CanESM5 model. Figures 8 and 9 show that the HadGEM3-GC3.1-LL model follows the same trend as the CanESM5 model. Sea-ice

thickness is clearly decreasing, with the year of rapid descent being approximately 1975. The two models will be compared in the next section.

Comparison

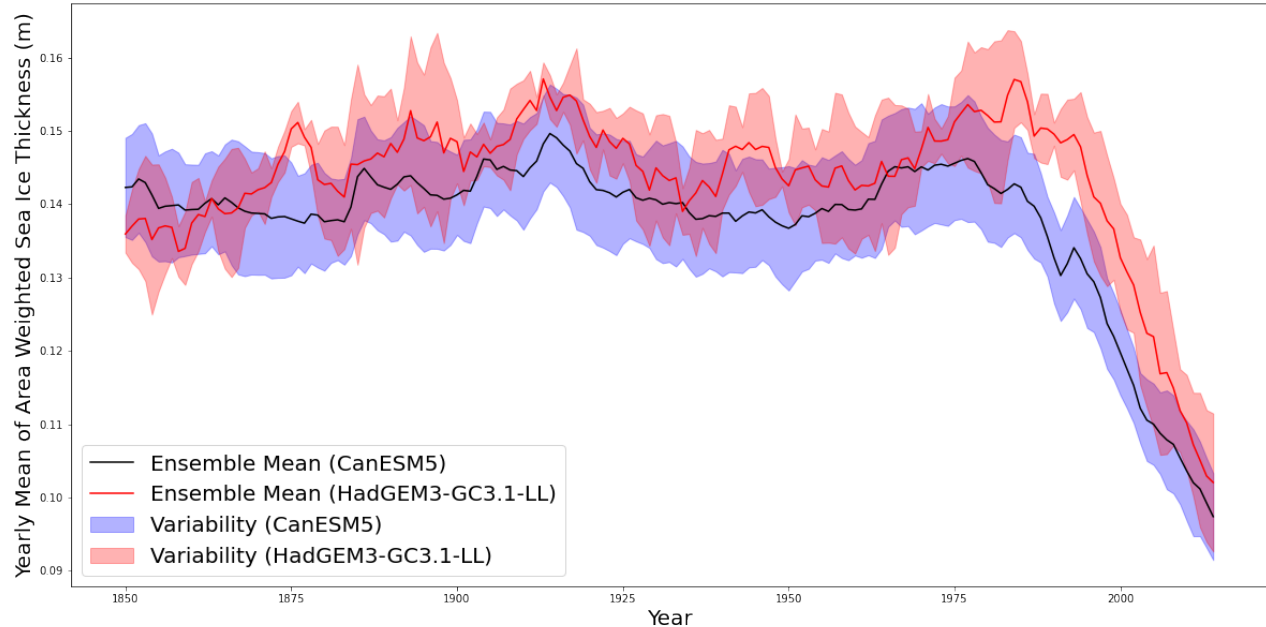


Figure 10: Qualitative Comparison of the CanESM5 model with the HadGEM3-GC3.1-LL model. Ensemble mean of area-weighted sea-ice thickness for areas north of the equator with sea-ice thickness above zero with shaded variability.

Figure 10 qualitatively compares the CanESM5 model to the HadGEM3-GC3.1-LL model. In both, the point where sea-ice thickness starts decreasing rapidly is 1975. On average, the CanESM5 model appears to project smaller yearly mean of area weighted sea-ice thickness than the HadGEM3-GC3.1-LL model. Without a comparison to observations, it is impossible to state whether one model is more accurate than the other, rather the comparison is just based on how the two compare against each other. To quantitatively compare these diagrams, Taylor diagrams were used.

Without observations, a way to compare the two models is to choose one of the CanESM5 ensemble members as the reference dataset. This reference is compared to five additional ensemble members within CanESM5, as well as one ensemble member from the HadGEM3-GC3.1-LL model. For the historic simulations, two different ensemble members from the CanESM5 model were set as the reference data-set to produce two Taylor diagrams. As well, two different ensemble member from the HadGEM3-GC3.1-LL model were compared to the CanESM5 model. This was done to

ensure that the results from the Taylor diagrams are representative of the models as a whole, rather than only one ensemble member.

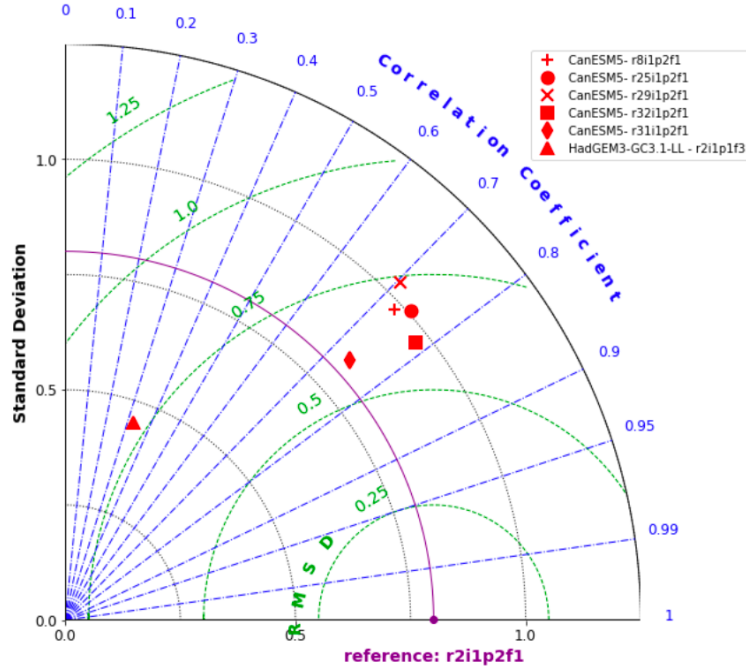


Figure 11: Taylor diagram comparing CanESM5 reference model (r2i1p1f1) to five ensemble members from the CanESM5 model and one ensemble member (r2i1p1f3) from the HadGEM3-GC3.1-LL model in 2014.

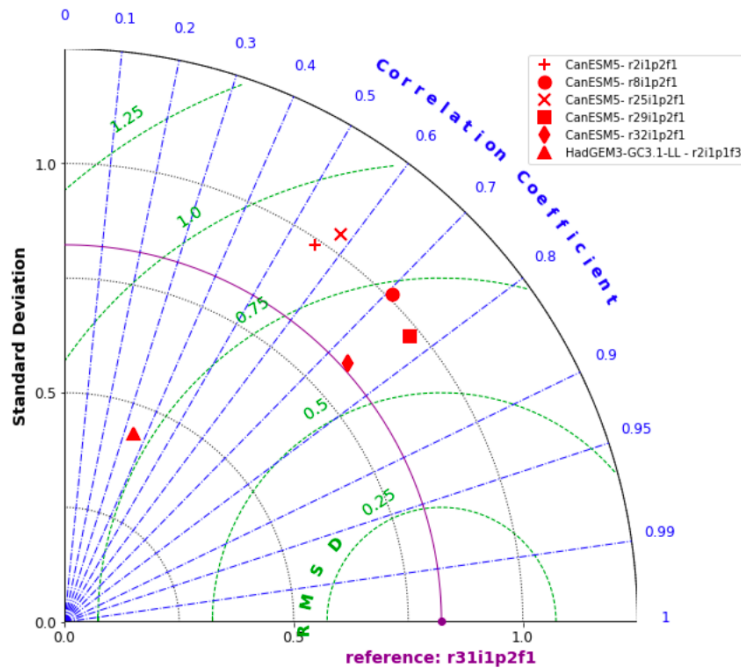


Figure 12: Taylor diagram comparing CanESM5 reference model (r3i1p2f1) to five ensemble members from the CanESM5 model and one ensemble member (r2i1p1f3) from the HadGEM3-GC3.1-LL model in 2014.

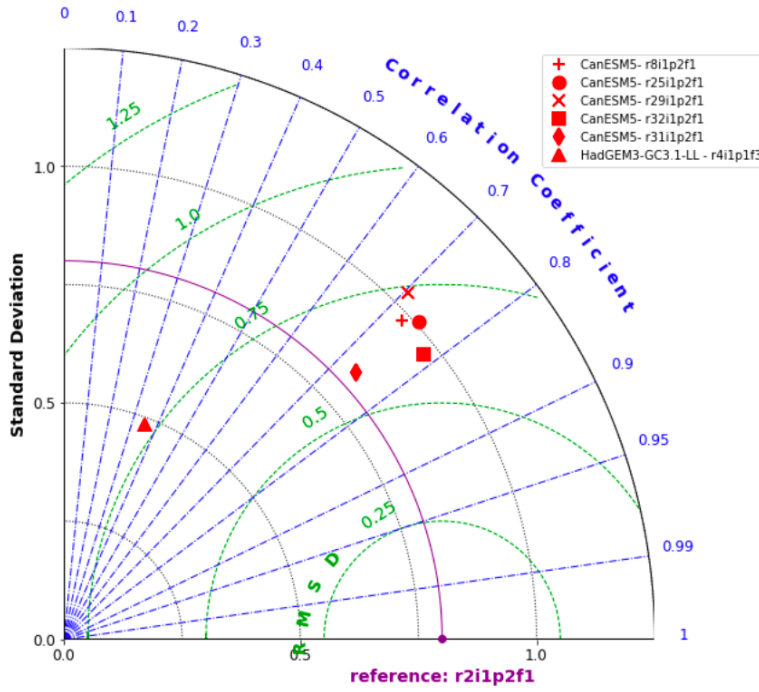


Figure 13: Taylor diagram comparing CanESM5 reference model (r2i1p1f1) to five ensemble members from the CanESM5 model and one ensemble member (r4i1p1f3) from the HadGEM3-GC3.1-LL model in 2014.

Figures 11, 12, and 13 compare historical simulations of sea-ice thickness from the CanESM5 and HadGEM3-GC3.1-LL models in 2014. This date was chosen to compare the two models at a time that is near the present-day. Figures 11 and 12 compare the same ensemble member from the HadGEM3-GC3.1-LL model against different ensemble members within the Canadian model in 2014. The legends outlines which ensemble members are being compared. Figure 13 compares the same 5 Canadian ensemble member against the same reference ensemble member as Figure 11 with a different ensemble member from the HadGEM3-GC3.1-LL model, again in 2014.

In Figure 11 the ensemble members from the CanESM5 model are clustered together. Their correlation coefficients are an average of 0.7 with the reference dataset. The ensemble member from the HadGEM3-GC3.1-LL model has a correlation coefficient of about 0.3 with the reference dataset from the CanESM5 model. The smaller standard deviation that is visible with the HadGEM3-GC3.1-LL model ensemble member is because the ensemble member has less variability within it than the CanESM5 ensemble members. Figure 12 is quite similar to Figure 11. The ensemble members from the CanESM5 model are less clustered than the previous figure, and their correlations range from 0.5 to 0.8. The ensemble member from the HadGEM3-GC3.1-LL model has a correlation coefficient of about 0.3. Figure 13 is identical to Figure 11 with respect to the CanESM5 ensemble members. This ensemble member from the HadGEM3-GC3.1-LL model acts very similarly to the previous ensemble member that was compared. Overall, we can tell quantitatively that the CanESM5 and HadGEM3-GC3.1-LL models behave differently. The correlation coefficient is much smaller between models than it is within

models. These Taylor diagrams confirm that there is a difference between the models in the historical simulations. To further examine their differences, Taylor diagrams were created for the two future emissions scenarios: SSP2-4.5 and SSP5-8.5 in 2031.

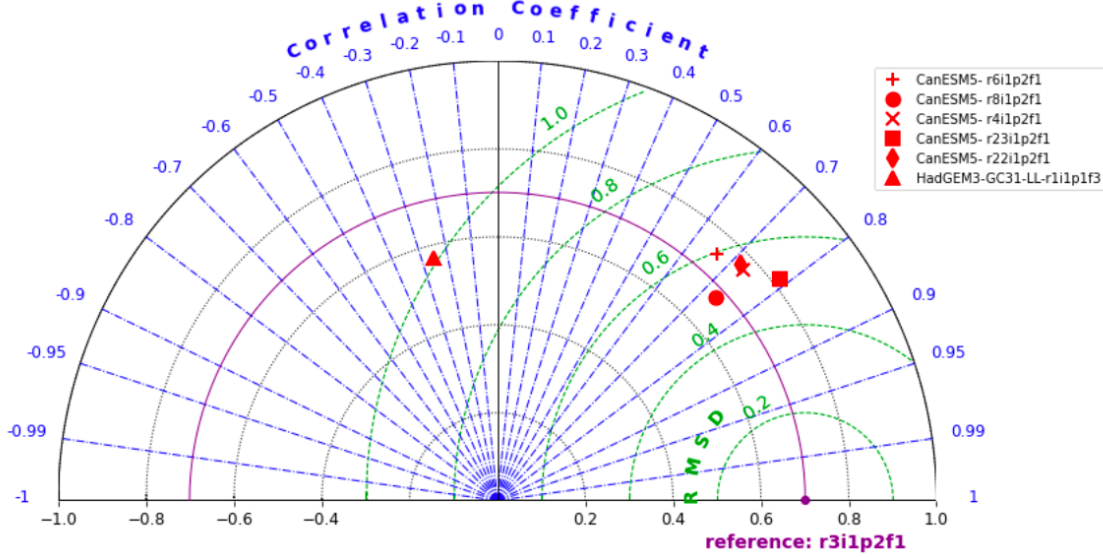


Figure 14: Taylor diagram comparing CanESM5 reference model (r3i1p2f1) to five ensemble members from the CanESM5 model and one ensemble member (rii1p1f3) from the HadGEM3-GC3.1-LL model in the SSP2-4.5 emissions scenario in 2031.

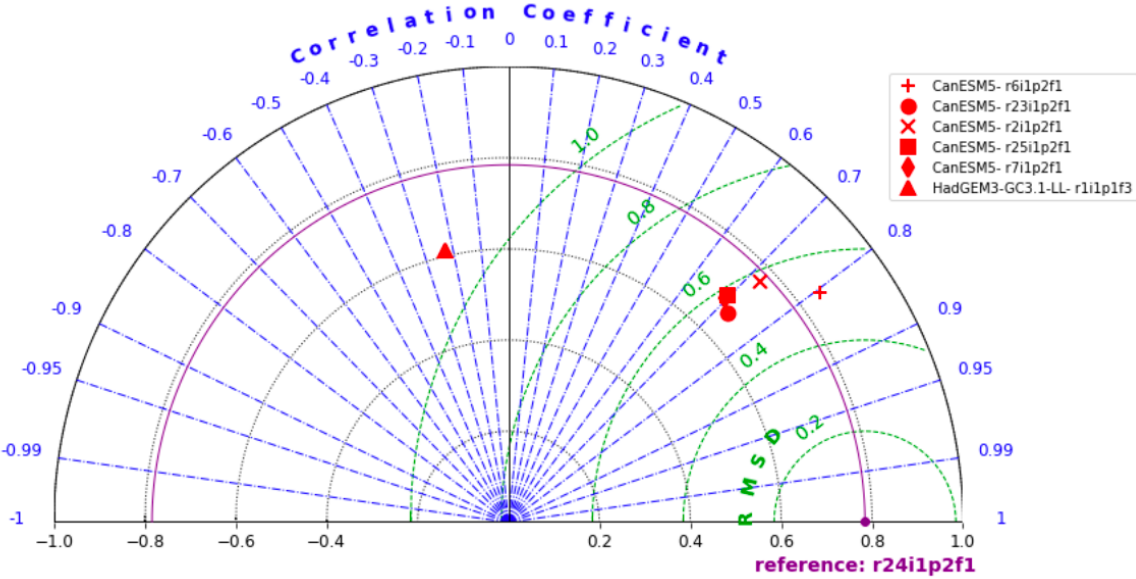


Figure 15: Taylor diagram comparing CanESM5 reference model (r24i1p2f1) to five ensemble members from the CanESM5 model and one ensemble member (rii1p1f3) from the HadGEM3-GC3.1-LL model in the SSP5-8.5 emissions scenario in 2031.

Figures 14 and 15 are Taylor diagrams for the two emissions scenarios that have been focused on throughout this project, in 2031. The double-sided Taylor diagram is used in

these two emissions scenarios because the HadGEM3-GC3.1-LL ensemble member has negative correlation to the CanESM5 ensemble member that is acting as the reference dataset. These Taylor diagrams confirm that the two models are different in their future emissions scenarios.

The Taylor diagrams presented above determine that there are definitive and clear differences between the two sea-ice thickness models. This could be due to the different atmosphere and ocean models that are used within the sea-ice thickness models. It could also be due to the different couplers that are used, or the different initial conditions.

Conclusion

Within both the historic simulations of CanESM5 and HadGEM3-GC3.1-LL sea-ice thickness begins to dramatically decrease around 1975. From there, the sea-ice decreases until the last time-step of the historic simulation, in 2014. The future emissions scenarios SSP2-4.5 and SSP5-8.5 simulate a continuing trend of decreasing sea-ice thickness until the end of the century. If the worst case scenario (SSP5-8.5) comes to fruition, by 2100, there will hardly be any sea-ice left in the arctic.

The Taylor diagrams for both the historical simulations and the future emissions scenarios show that the CanESM5 model differs from the HadGEM3-GC3.1-LL model. The ensemble members within the CanESM5 model have much higher correlation coefficients to the reference ensemble member. This could be for a variety of reasons. The two models were created by different modelling institutions. Each institution has a different team of scientists that developed each model, with varying assumptions and decisions made. The two models use different atmosphere models, and versions of the NEMO ocean configuration optimized in a potentially different manner for each model.

Through qualitative and quantitative analyses of the sea-ice thickness models, it is clear that the CanESM5 model, as well as the HadGEM3-GC3.1-LL model project further decreases in sea ice thickness in the arctic. It is not possible at this time to make definitive statements on the accuracy of the two models or determine which model performed better, without a comparison of both models to a set of observations. In the future, these models could be compared against sea-ice thickness observations to determine which model is more accurate. Replacing the reference ensemble member with a reference set of observations would change the Taylor diagrams from simply comparing two sea-ice thickness models, to determining which is more accurate.

References

- Andrews, M. B., Ridley, J. K., Wood, R. A., Andrews, T., Blockley, E. W., Booth, B., Burke, E., Dittus, A. J., Florek, P., Gray, L. J., Haddad, S., Hardiman, S. C., Hermanson, L., Hodson, D., Hogan, E., Jones, G. S., Knight, J. R., Kuhlbrodt, T., Misios, S., ... Sutton, R. T. (2020). Historical Simulations With HadGEM3-GC3.1 for CMIP6. *Journal of Advances in Modeling Earth Systems*, 12(6), e2019MS001995. <https://doi.org/https://doi.org/10.1029/2019MS001995>
- Bengtsson, L., & Hodges, K. I. (2019). Can an ensemble climate simulation be used to separate climate change signals from internal unforced variability? *Climate Dynamics*, 52(5), 3553–3573. <https://doi.org/10.1007/s00382-018-4343-8>
- CMIP6: the next generation of climate models explained.* (2019, December 2). Carbon Brief. <https://www.carbonbrief.org/cmip6-the-next-generation-of-climate-models-explained>
- Hunter, J. D. (2007). Matplotlib: A 2D graphics environment. *Computing in Science & Engineering*, 9(3), 90–95.
- Notz, D., & Community, S. (2020). Arctic Sea Ice in CMIP6. *Geophysical Research Letters*, 47(10). <https://doi.org/10.1029/2019GL086749>
- Panikkar, B., & Lemmond, B. (2020). Being on Land and Sea in Troubled Times: Climate Change and Food Sovereignty in Nunavut. *Land*, 9(12), 508. <https://doi.org/10.3390/land9120508>
- Pickart, R. S. (2018). Climate Change at High Latitudes: An Illuminating Example. *Zygon®*, 53(2), 496–506. <https://doi.org/https://doi.org/10.1111/zygo.12406>
- Riahi, K., Rao, S., Krey, V., Cho, C., Chirkov, V., Fischer, G., Kindermann, G., Nakicenovic, N., & Rafaj, P. (2011). RCP 8.5—A scenario of comparatively high greenhouse gas emissions. *Climatic Change*, 109(1), 33. <https://doi.org/10.1007/s10584-011-0149-y>
- Ridley, J. K., Blockley, E. W., Keen, A. B., Rae, J. G. L., West, A. E., & Schroeder, D. (2018). The sea ice model component of HadGEM3-GC3.1. *Geoscientific Model Development*, 11(2), 713–723. <https://doi.org/https://doi.org/10.5194/gmd-11-713-2018>

Rochford, P. (2021). PeterRochford/SkillMetricsToolbox (<https://github.com/PeterRochford/SkillMetricsToolbox>), GitHub. Retrieved April 24, 2021.

Swart, N. C., Cole, J. N. S., Kharin, V. V., Lazare, M., Scinocca, J. F., Gillett, N. P., Anstey, J., Arora, V., Christian, J. R., Hanna, S., Jiao, Y., Lee, W. G., Majaess, F., Saenko, O. A., Seiler, C., Seinen, C., Shao, A., Sigmond, M., Solheim, L., ... Winter, B. (2019). The Canadian Earth System Model version 5 (CanESM5.0.3). *Geoscientific Model Development*, 12(11), 4823–4873. <https://doi.org/https://doi.org/10.5194/gmd-12-4823-2019>

Taylor, K. E. (2001). Summarizing multiple aspects of model performance in a single diagram. *Journal of Geophysical Research: Atmospheres*, 106(D7), 7183–7192. <https://doi.org/https://doi.org/10.1029/2000JD900719>

Thomson, A. M., Calvin, K. V., Smith, S. J., Kyle, G. P., Volke, A., Patel, P., Delgado-Arias, S., Bond-Lamberty, B., Wise, M. A., Clarke, L. E., & Edmonds, J. A. (2011). RCP4.5: a pathway for stabilization of radiative forcing by 2100. *Climatic Change*, 109(1), 77. <https://doi.org/10.1007/s10584-011-0151-4>

Wei, T., Yan, Q., Qi, W., Ding, M., & Wang, C. (2020). Projections of Arctic sea ice conditions and shipping routes in the twenty-first century using CMIP6 forcing scenarios. *Environmental Research Letters*, 15(10), 104079. <https://doi.org/10.1088/1748-9326/abb2c8>

Williams, K. D., Copsey, D., Blockley, E. W., Bodas-Salcedo, A., Calvert, D., Comer, R., Davis, P., Graham, T., Hewitt, H. T., Hill, R., Hyder, P., Ineson, S., Johns, T. C., Keen, A. B., Lee, R. W., Megann, A., Milton, S. F., Rae, J. G. L., Roberts, M. J., ... Xavier, P. K. (2018). The Met Office Global Coupled Model 3.0 and 3.1 (GC3.0 and GC3.1) Configurations. *Journal of Advances in Modeling Earth Systems*, 10(2), 357–380. <https://doi.org/https://doi.org/10.1002/2017MS001115>